Materials Letters 210 (2018) 186–190

Contents lists available at ScienceDirect

Materials Letters

journal homepage: www.elsevier.com/locate/mlblue

Novel porous bioabsorbable phosphate glass matrix nanocomposites incorporating trisilanolphenyl polyhedral oligomeric silsesquioxane prepared by extrusion

Kyoungtae Kim, Imane Belyamani, Joshua U. Otaigbe *

School of Polymers and High Performance Materials, The University of Southern Mississippi, 118 College Drive, Hattiesburg, MS 39406, United States

ARTICLE INFO

Article history:
Received 18 April 2017
Received in revised form 22 August 2017
Accepted 2 September 2017
Available online 6 September 2017

Keywords:
Glass matrix composites
Extrusion
Tin fluorophosphate glass
Polyhedral oligomeric silsesquioxane
Inorganic foams

ABSTRACT

Phosphate glass matrix nanocomposites containing trisilanolphenyl polyhedral oligomeric silsesquioxane (POSS) were investigated for the first time to accelerate efforts to develop novel hybrid phosphate glass/POSS composites with enhanced benefits. Tin fluorophosphate glass (Pglass) having ultra-low glass transition temperature (T_g) was utilized as the matrix material in extrusion at relatively low processing temperature (i.e., 270 ± 10 °C) compared to that of typical borosilicate and sodalime glasses. The resulting nanocomposites materials were highly porous due to evaporation of condensed water produced *in situ* from polysiloxane condensation reaction between the Pglass and POSS during the extrusion process. As the amount of POSS was increased in the Pglass matrix material, the glass transition temperature was significantly changed by the bulky POSS molecules. The novel porous nanocomposites should find a number of uses in applications at elevated temperatures where conventional organic polymer foam materials are not useable.

1. Introduction

While novel bioabsorbable phosphate glass-polymer composites [1] and porous scaffolds [2,3] with enhanced benefits have been reported in the literature, to our knowledge, the work described in this article is the first reported study that demonstrated feasibility of making porous glass matrix nanocomposites using extrusion processing (traditionally used for organic polymer processing) that takes advantage of the relative low-cost and high efficiency in distributing the nanofiller materials in the glass matrix materials [4]. The improved nanofiller dispersion of the trisilanolphenyl polyhedral oligomeric silsesquioxane (TSP-POSS) used here translates to an increase in interfacial surface area of the nanocomposite and improved nano-reinforcement and biomedical function [5]. Other researchers have reported borosilicate glass matrix composites [6] and porous glass foam materials with uses in membrane, catalyst and biotechnology applications with improved properties [7].

In the current study, TSP-POSS was incorporated for the first time into a phosphate glass (Pglass) matrix to yield functional micro(nano)structured porosity without using foaming agents such as calcium carbonate to generate the gas phase during the processing [8]. It is worthy to note that phosphate glass was selected for this study because it is the lowest glass transition temperature Pglass (*ca.* ~100 °C) with optimal combination of water resistance and desirable rheological characteristics, as well as, complete and congruent biodegradation and biocompatibility as previously reported [1,9].

2. Experimental

2.1. Materials

The Pglass was synthesized with a molar composition of $50SnF_2 + 20SnO + 30P_2O_5$ by heating, in a furnace maintained at 430 °C, a mixture of the stoichiometric amounts of the initial raw materials in an appropriate high-temperature crucible for 30 min [9].

Fig. 1 shows the chemical structures of Pglass and TSP-POSS. Pure Pglass and two different amounts of TSP-POSS (~10 wt%) were used and manually mixed using a mortar and pestle. Trisilanol phenyl POSS (TSP-POSS, $C_{42}H_{38}O_{12}Si_7$, Hybrid Plastics) was used. Analytical grade reagents, Tin(II) oxide (SnO), tin(II) fluoride (SnF_2), ammonium dihydrogen phosphate ($(NH_4)H_2PO_4$) were purchased from Sigma-Aldrich and used as received.

* Corresponding author.
E-mail address: Joshua.Otaigbe@usm.edu (J.U. Otaigbe).

http://dx.doi.org/10.1016/j.matlet.2017.09.016
0167-577X/

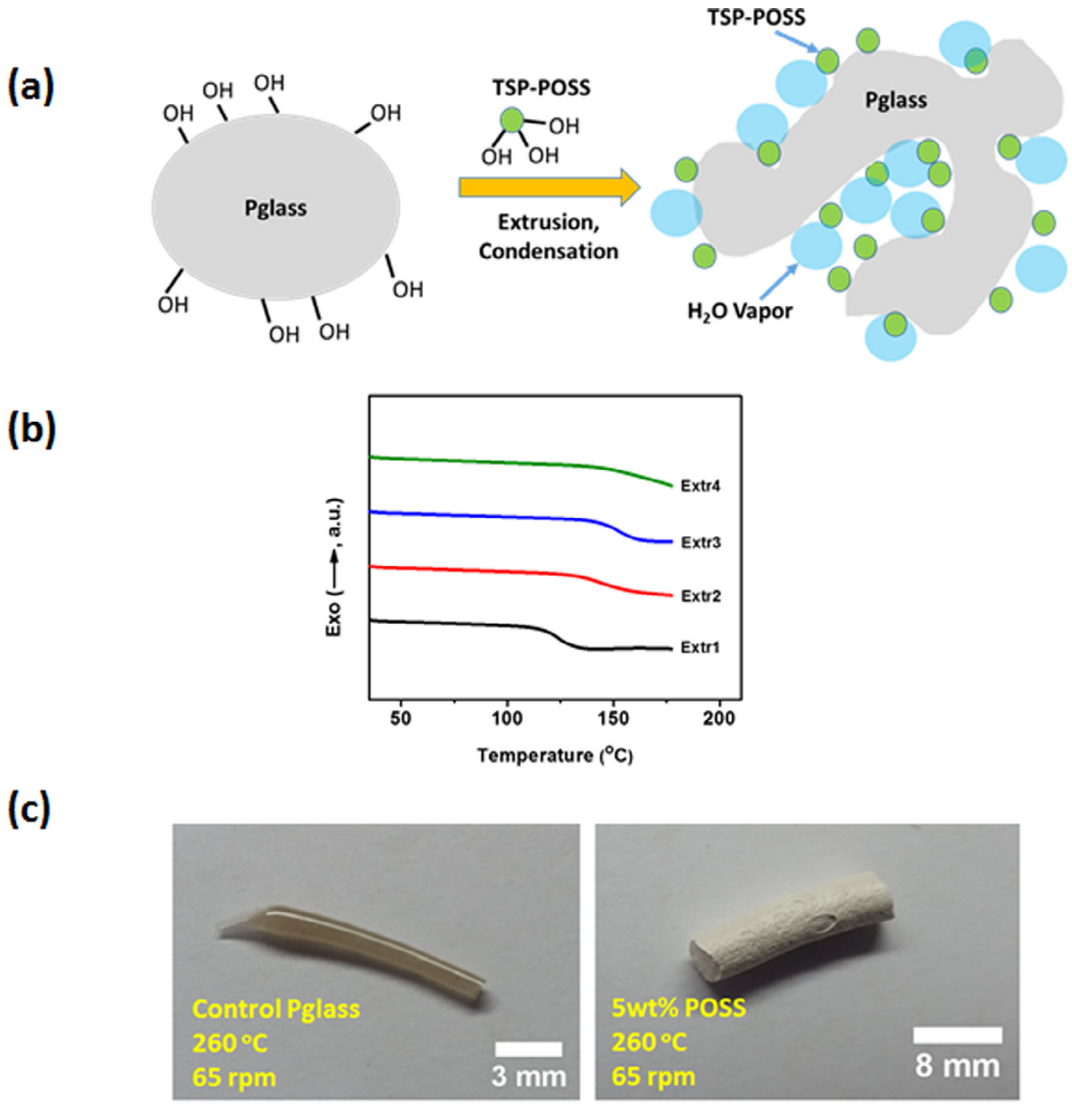

Fig. 1. (a) The expected macroscopic structure, (b) DSC thermograms, and (c) pictures of Pglass/TSP-POSS nanocomposites prepared by extrusion.

2.2. Extrusion processing

The desired amount of Pglass powder and POSS powder was mixed manually and continuously introduced into the feed-throat of a MiniLab® twin-screw extruder and conveyed by the extruder screws through the extruder slit die of 1 mm diameter to yield the glass matrix nanocomposite containing POSS as presented in details in Supplementary information.

2.3. Measurements

T_g was characterized by standard differential thermal analysis (PerkinElmer Pyris Diamond® DSC) under dry nitrogen atmosphere from 30 °C to 180 °C, 10 °C/min rate. Standard SEM-EDX analysis was used to investigate the morphology and elemental compositions of the samples. Standard ^{31}P NMR, solid-state NMR, and solid-state CP/MAS ^{29}Si NMR spectroscopy were used to characterize the chemical structure and dynamics of the samples as presented in details in the Supplementary information. The porosity of samples was estimated by comparing measured density to theoretical density of the samples.

3. Results and discussion

Fig. 1(a) illustrates how the TSP-POSS was dispersed in Pglass matrix via mechanical mixing and hydrogen bonding in the extrusion process, allowing condensation reaction between TSP-POSS and Pglass and between two of each material, that produced water vapor inside of the Pglass matrix, transforming into homogeneous porosity in the nanocomposites. As the amount of POSS was increased in the Pglass matrix materials, the T_g increased until it finally disappeared as shown in Table 1. This observation suggests that either the glass changed to a glass-ceramic or the T_g value of nanocomposites probably occurred at higher temperature, where thermal degradation prevented its determination. The obtained results suggest that mobility of the Pglass chains is restricted by the addition of the relatively bulky POSS molecules, leading to a decrease of mobility of the Pglass chains that was signaled by the observed increased T_g [10]. The extruded pure Pglass and nanocomposites materials are shown in Fig. 1(c).

The molecular structure and miscibility of the nanocomposites and its constituents were analyzed via solid-state NMR studies. ^{29}Si CPMAS NMR was conducted to obtain the local structural information between the Pglass and pure POSS as shown in Fig. 2(a). This

Table 1
Glass transition temperature (T_g), density, porosity, and the deconvolution of ^{31}P DP/MAS solid-state NMR data on pure Pglass and nanocomposites prepared by the extrusion method.

Sample	DSC	NMR		Measured Density (g/cm^3)	Theoretical Density (g/cm^3)	Porosity (%)
	T_g (°C)	Q^0	Q^1			
Extr1	124.2 ± 0.8	22.0 ± 1	78.0 ± 1	3.39 ± 0.07	3.75	9.7 ± 1.9
Extr2	146.3 ± 1.3	27.3 ± 1	72.7 ± 1	0.65 ± 0.03	3.63	82.2 ± 0.8
Extr3	151.0 ± 0.9	28.5 ± 1	71.5 ± 1	0.71 ± 0.03	3.63	80.6 ± 0.8
Extr4	No T_g	37.1 ± 1	62.9 ± 1	0.85 ± 0.09	3.52	75.8 ± 2.4

Porosity = 1 − (measured density/theoretical density)) * 100.

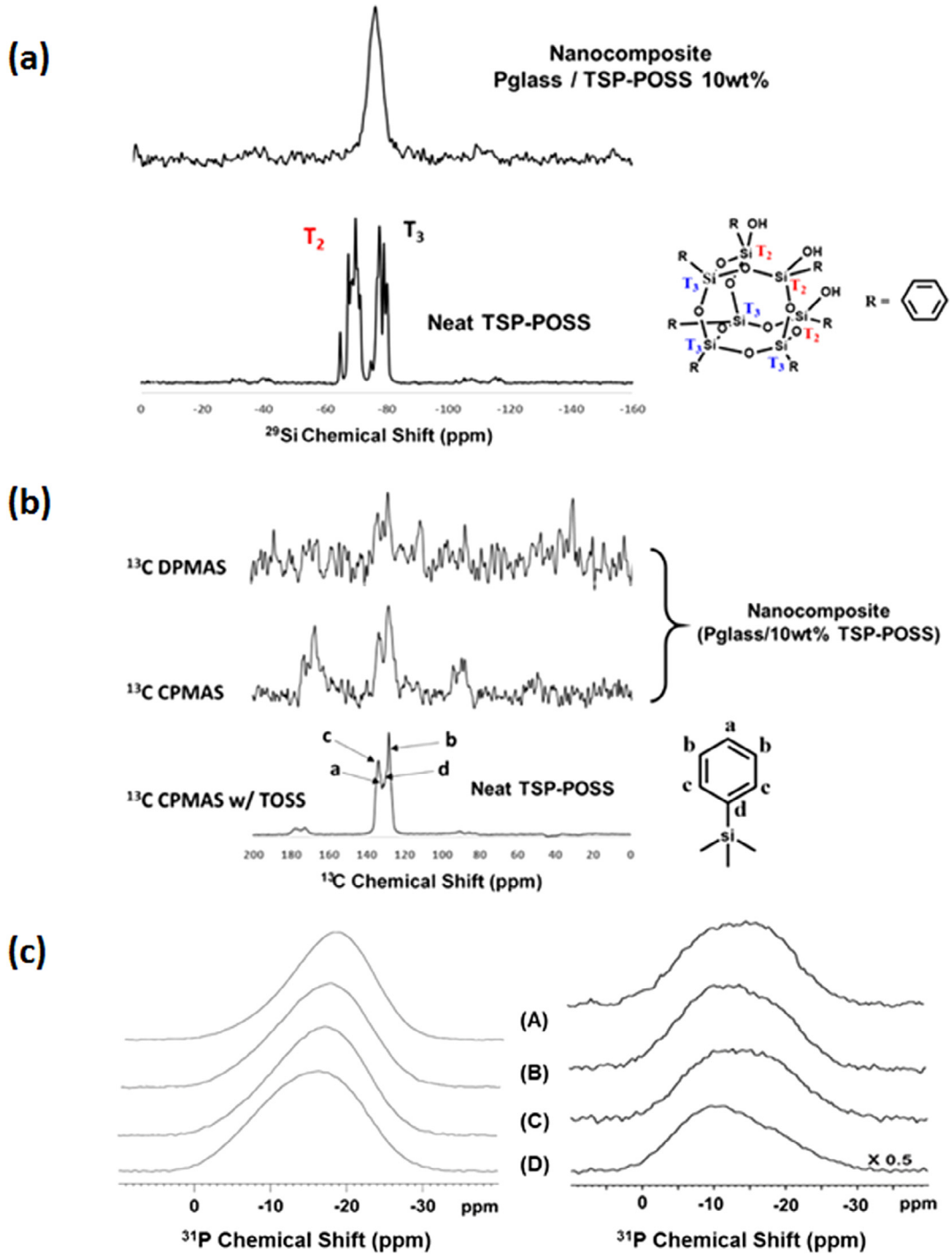

Fig. 2. (a) ^{29}Si spectra of TSP-POSS, (b) ^{13}C CP/MAS spectra of TSP-POSS and ^{13}C CP/MAS and DP/MAS spectra of Extr4 sample, and (c) ^{31}P DP/MAS (left) and ^{31}P CP/MAS (right) spectra in (A) Extr1, (B) Extr2, (C) Extr3, and (D) Extr4 samples in solid-state NMR analysis; (Extr1: pure Pglass with 260 °C/65 rpm, Extr2: 5 wt% POSS with 260 °C/65 rpm, Extr3: 5 wt% POSS with 280 °C/80 rpm, Extr4: 10 wt% POSS with 260 °C/65 rpm).

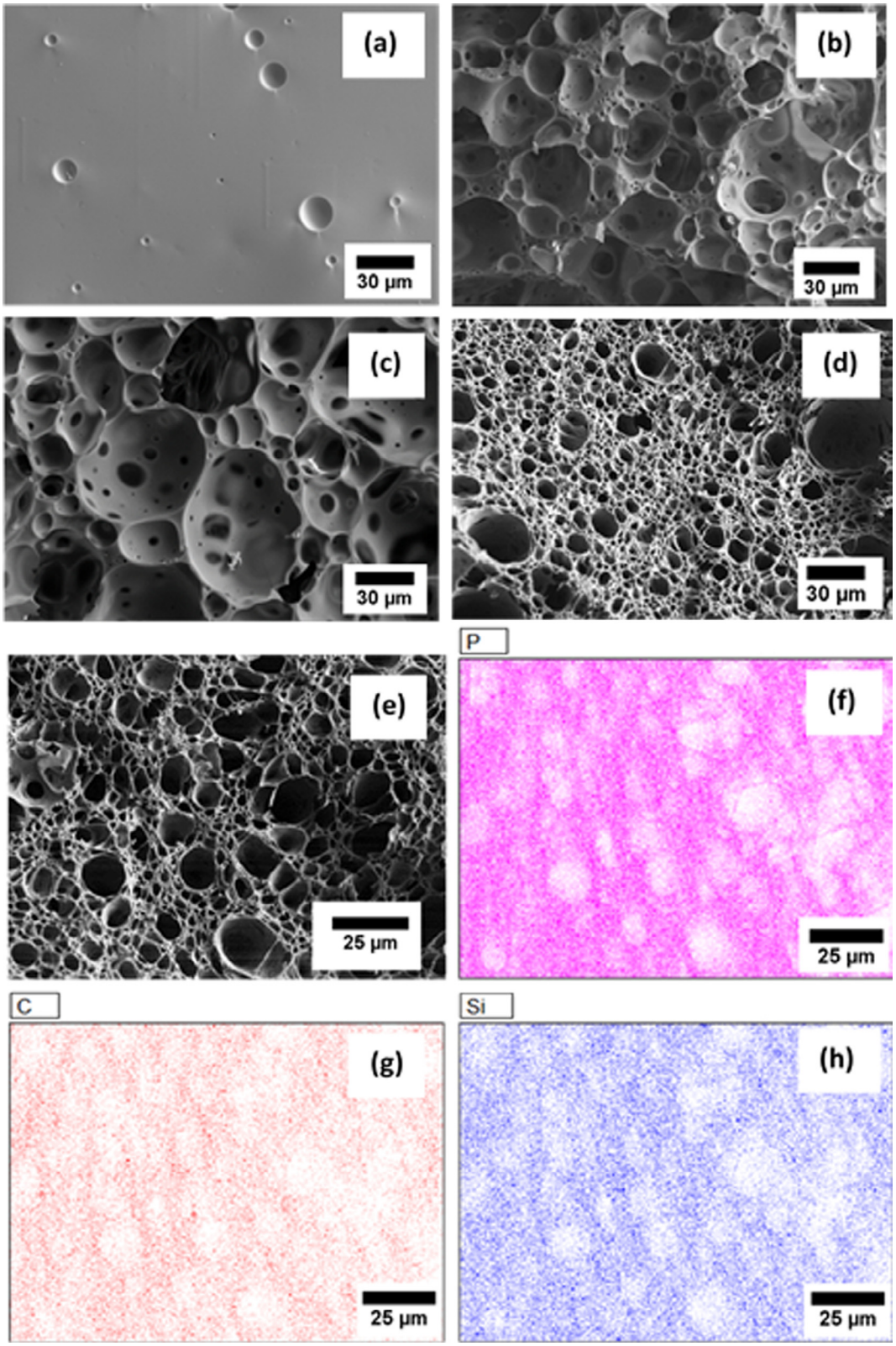

Fig. 3. SEM images of fracture surfaces of extruded Pglass and Pglass nanocomposite incorporating POSS: (a) Extr1, (b) Extr2, (c) Extr3 (d) Extr4, (e) SEM image and EDX mapping images of each element; (f) phosphorous, (g) carbon and (h) silicon in the 10 wt% POSS/Pglass matrix nanocomposite (white is background the color spots are elements in the EDX images shown in f, g, h).

figure shows that there are two sharp peak areas between −64 ppm and −82 ppm corresponding to T_2 and T_3 sites, indicating silicon connected to hydroxyl group (i.e., opened silicon) and silicon unconnected to hydroxyl group (i.e., closed silicon), respectively [11]. Disappearance of T_2 and the peak around −80 ppm are attributed to disappearance of silanol groups via condensation reactions between the nanocomposites constituents. In addition, the ^{29}Si spectra considerably broadened due to the reduction of

crystallinity of POSS caused by molecular-level dispersion in the nanocomposites. The ^{13}C spectra shown in Fig. 2(b) indicate sharp signals corresponding to four phenyl carbons at para (a, 132 ppm), meta (b, 128 ppm), ortho (c, 136 ppm) positions, and phenyl carbon attached to silicon oxide moiety of the POSS cage (d, 130 ppm) in the pure POSS [11]. In contrast, the broad signal shown in the nanocomposites samples indicates a reduction of crystallinity and homogeneous dispersion of POSS throughout the Pglass matrix.

The stack plot of the isotropic resonance shift obtained from DP/MAS and CP/MAS in ^{31}P NMR for the extruded nanocomposites is shown in Fig. 2(c). Upon addition of the TSP-POSS in the Pglass matrix, the ratio of Q^0 to Q^1 (where the numbers 0 and 1 indicate the number of bridging oxygen connected to phosphorous in the Pglass structure) increased as shown in Table 1, indicating that the Pglass chains changed from pyrophosphate to orthophosphate due to the addition of TSP-POSS [9]. Note that for the Pglass nanocomposites containing identical TSP-POSS concentration, changing the extrusion processing conditions did not reveal a significant shift of isotropic resonance in ^{31}P NMR, indicating that the effect on the Pglass structure of the amount of TSP-POSS used is more significant compared to that of the change of extrusion processing conditions used.

The fracture surface of the extruded pure Pglass showed little bubbles (or voids) caused by evaporation of bound water and entrapped air during the extrusion process as shown in Fig. 3(a). The nanocomposites contained relatively more porosity (Table 1) that was augmented by increased amount of POSS as shown in Fig. 3(b–d) due to *in situ* condensation reaction between the nanocomposites constituents [12]. Fig. 3(e–h) shows the distribution of each element in the samples characterized via SEM-EDX analysis on the fracture surface of the extruded nanocomposites incorporating 10 wt% POSS. Clearly, the phosphorous from Pglass and the carbon and silicon from TSP-POSS are distributed homogeneously in the nanocomposite samples in nanoscale.

4. Conclusions

This study demonstrates for the first time the feasibility of facile preparation of highly porous Pglass matrix nanocomposites incorporating POSS by extrusion processing. The significant porosity in the samples is ascribed to evaporation of *in situ* condensed water between hydroxyl groups of the Pglass and POSS during the extrusion process. The solid-state NMR data analysis confirmed the chemical functionality of the porous POSS/Pglass nanocomposites, excellent dispersion of the POSS, and associated increase in the interactions between the Pglass and POSS in the new nanocomposites with enhanced benefits in a wide range of potential applications such as biomedical and tissue engineering, heterogeneous catalysis, membrane, and composites, where existing materials cannot be used.

Acknowledgements

This work was supported by the U.S. National Science Foundation through DMR-1360006 award. We thank Jessica Douglas (SEM), William Jarrett (NMR), Todd Alam (NMR), and Hybrid Plastics Inc. for their technical assistance.

Appendix A. Supplementary data

Supplementary data associated with this article can be found, in the online version, at http://dx.doi.org/10.1016/j.matlet.2017.09.016.

References

[1] K. Urman, J.U. Otaigbe, New phosphate glass/polymer hybrids – current status and future prospects, Prog. Poly. Sci. 32 (12) (2007) 1462–1498.
[2] P. Gentile et al., Bioresorbable glass effect on the physico-chemical properties of bilayered scaffolds for osteochondral regeneration, Mater. Lett. 89 (2012) 74–76.
[3] G. Georgiou et al., Polylactic acid–phosphate glass composite foams as scaffolds for bone tissue engineering, J. Biomed. Mater. Res. Part B: Appl. Biomater. 80 (2) (2007) 322–331.
[4] E. Roeder, Extrusion of glass, J. Non-Cryst. Solids 5 (5) (1971) 377–388.
[5] S.A. Madbouly, J.U. Otaigbe, Recent advances in synthesis, characterization and rheological properties of polyurethanes and POSS/polyurethane nanocomposites dispersions and films, Prog. Poly. Sci. 34 (12) (2009) 1283–1332.
[6] E. Minay, V. Desbois, A. Boccaccini, Innovative manufacturing technique for glass matrix composites: extrusion of recycled TV set screen glass reinforced with Al 2 O 3 platelets, J. Mater. Proc. Technol. 142 (2) (2003) 471–478.
[7] E. Boccardi, F.E. Ciraldo, A.R. Boccaccini, Bioactive glass-ceramic scaffolds: processing and properties, MRS Bull. 42 (3) (2017) 226–232.
[8] B. Chen et al., Study of foam glass with high content of fly ash using calcium carbonate as foaming agent, Mater. Lett. 79 (2012) 263–265.
[9] K. Kim et al., Synthesis and characterization of novel phosphate glass matrix nanocomposites containing polyhedral oligomeric silsesquioxane with improved properties, J. Non-Cryst. Solids 463 (2017) 189–202.
[10] G. Li et al., Polyhedral oligomeric silsesquioxane (poss) polymers and copolymers: a review, J. Inorg. Org. Poly. 11 (3) (2001) 123–154.
[11] R. Misra et al., Molecular miscibility and chain dynamics in POSS/polystyrene blends: control of POSS preferential dispersion states, Polymer 50 (13) (2009) 2906–2918.
[12] A.G. Kannan, N.R. Choudhury, N.K. Dutta, Synthesis and characterization of methacrylate phospho-silicate hybrid for thin film applications, Polymer 48 (24) (2007) 7078–7086.